

X-RAYS IN CEPHEIDS: IDENTIFYING LOW-MASS COMPANIONS OF INTERMEDIATE-MASS STARS ^a

NANCY REMAGE EVANS

Smithsonian Astrophysical Observatory, MS 4, 60 Garden St., Cambridge, MA 02138; nevens@cfa.harvard.edu

SCOTT ENGLE

Department of Astronomy and Astrophysics, Villanova University, 800 Lancaster Ave., Villanova, PA, 19085, USA

IGNAZIO PILLITTERI

INAF-Osservatorio di Palermo, Piazza del Parlamento 1,I-90134 Palermo, Italy

EDWARD GUINAN

Department of Astronomy and Astrophysics, Villanova University, 800 Lancaster Ave., Villanova, PA, 19085, USA

H. MORITZ GÜNTHER

Massachusetts Institute of Technology, Kavli Institute for Astrophysics and Space Research, 77 Massachusetts Ave, NE83-569, Cambridge MA 02139, USA

SCOTT WOLK

Smithsonian Astrophysical Observatory, MS 4, 60 Garden St., Cambridge, MA 02138

HILDING NEILSON

Department of Astronomy and Astrophysics, University of Toronto, 50 St. George Street, Toronto, ON, Canada M5S3H4

MASSIMO MARENGO

Department of Physics and Astronomy, Iowa State University, Ames, IA, 50011, USA

LYNN D. MATTHEWS

Massachusetts Institute of Technology, Haystack Observatory, 99 Millstone Rd., Westford, MA 01886, USA

SOFIA MOSCHOU

Smithsonian Astrophysical Observatory, MS 4, 60 Garden St., Cambridge, MA 02138

JEREMY J. DRAKE

Smithsonian Astrophysical Observatory, MS 4, 60 Garden St., Cambridge, MA 02138

ELAINE M. WINSTON

Smithsonian Astrophysical Observatory, MS 4, 60 Garden St., Cambridge, MA 02138; nevens@cfa.harvard.edu

^a Based on observations obtained with the Chandra X-ray Observatory

MAXWELL MOE

University of Arizona, Steward Observatory, 933 N. Cherry Ave., Tucson, AZ 85721, USA

PIERRE KERVELLA

LESIA, Observatoire de Paris, Université PSL, CNRS, Sorbonne Université, Université de Paris, 5 Place Jules Janssen, 92195 Meudon, France

LOUISE BREUVAL

LESIA, Observatoire de Paris, Université PSL, CNRS, Sorbonne Université, Université de Paris, 5 Place Jules Janssen, 92195 Meudon, France
and

Department of Physics and Astronomy, Johns Hopkins University, Baltimore, MD 21218, USA

ABSTRACT

X-ray observations have been made of a sample of 20 classical Cepheids, including two new observations (Polaris and l Car) reported here. The occurrence of X-ray flux around the pulsation cycle is discussed. Three Cepheids are detected (δ Cep, β Dor, and Polaris). X-rays have also been detected from the low-mass F, G, and K companions of 4 Cepheids (V473 Lyr, R Cru, V659 Cen, and W Sgr), and one hot companion (S Mus). Upper limits on the X-ray flux of the remaining Cepheids provide an estimate that 28% have low mass companions. This fraction of low-mass companions in intermediate mass Cepheids is significantly lower than expected from random pairing with the field IMF. Combining the companion fraction from X-rays with that from ultraviolet observations results in a binary/multiple fraction of $57\% \pm 12\%$ for Cepheids with the ratios $q > 0.1$ and separations $a > 1$ au. This is a lower limit since M stars are not included. X-ray observations detect less massive companions than other existing studies of intermediate mass stars. Our measured occurrence rate of unresolved, low-mass companions to Cepheids suggests that intermediate-period binaries derive from a combination of disk and core fragmentation and accretion. This yields a hybrid mass-ratio distribution that is skewed toward small values compared to a uniform distribution but is still top-heavy compared to random pairings drawn from the IMF.

Keywords: stars: Cepheids; binaries; stars:massive; stars: variable; X-rays; star formation

1. INTRODUCTION

Massive and intermediate mass stars typically form as members of a pair or group. This is an important aspect, for instance, of the evolution of angular momentum in the pre-main sequence phase. Many exotic objects in later phases of evolution arise from the combination of a compact object in a binary or multiple system. For example, this combination produces core collapse supernovae and even gravitational wave systems. Cepheids are most commonly approximately $5 M_{\odot}$ stars, intermediate mass stars rather than a high mass stars. They typically ultimately become white dwarfs, although the most massive may become neutron stars. However, their binary/multiple characteristics are similar to those of more massive stars, and can provide insight into evolution past the main sequence. Cepheid progenitors are B stars. Banyard, et al (2021) provide a recent summary of B star binary properties for comparison with Cepheid properties.

Components of stars in a multiple system can be challenging to disentangle. Intermediate mass Cepheids provide good examples of the many approaches needed to derive the masses and separations of the components. Radial velocity studies of spectroscopic binaries (Evans et al. 2015) and high resolution techniques provide basic information (Evans, et al. 2020a), supplemented by proper motions in the Gaia era (Kervella, et al. 2019 a, b). However, in multiple systems additional information is frequently needed to identify all the system components. For Cepheids, the fact that they have evolved into cool supergiants means it is possible to identify a complete list of hot companions in ultraviolet

spectra (Evans et al. 2013) with spectral types of B and early A (called “late B stars” below). Low mass companions, however, are more elusive, since the spectrum at ultraviolet, optical, and infrared wavelengths is dominated by the more luminous supergiant. X-rays provide a good remedy for this problem.

Cepheids, like other coronal supergiants (Engle 2015; Ayres 2011) produce a comparatively modest X-ray flux. δ Cep itself typically has an X-ray luminosity $\log L_X = 28.6$ ergs sec^{-1} . However, in an exciting development Engle et al. (2017) found a sharp increase in X-ray flux for a brief period near maximum radius in the pulsation cycle. This was seen in two pulsation cycles and also in the Cepheid β Dor.

Main sequence stars of spectral types F, G, and K at the age of Cepheids (typically 50 Myr), on the other hand are much more vigorous producers of X-rays. This makes X-rays a good discriminant between young physical companions of Cepheids and old field stars. Mapping the X-ray production of low-mass main sequence stars in temperature and age has been an important contribution of X-ray studies. We use this legacy to predict X-ray fluxes from possible companions at the age of Cepheids. Details are discussed in Section 4.4.

The vigorous X-ray production of low-mass main sequence stars adds an important piece to the determination of the properties of the multiple systems of Cepheids and other intermediate mass stars. X-ray observations of Cepheids where the upper limit is below the level of possible main sequence companions indicate that a low-mass companion is *not* present. This provides the fraction of Cepheid systems with low-mass companions. Since low-mass stars dominate the stellar mass distribution, identifying them is important for putting together a complete picture of star formation.

A thorough discussion of the observed properties of binary and multiple systems systems is given in Moe and Di Stefano (2017). In particular they discuss the distributions of mass ratios and separations as a function of mass of the primary and the implications for star formation. The distribution of mass ratios as a function of separation for O and B stars divides into 3 separation regimes. Close binaries with separations < 0.4 au favor reasonably massive companions, with $q = M_2/M_1 \simeq 0.5$. In this separation range presumably competitive accretion has resulted in relatively equal masses of the components. Stars in this separation range are not present in the Cepheid sample due to Roche lobe overflow (RLOF). Systems with wider separations up to 200 au tend to have smaller mass ratios $q \simeq 0.2$ to 0.3 . Companions at wider separations (200 to 5000 au) in O B systems tend to be outer components in triple systems. Their masses are close to a random pairing with the IMF, favoring low-mass companions. Fig. 1 in Moe and Di Stefano shows that the addition of systems with mass ratios q as small as 0.1 in the present study fills a gap for stars as massive as O and B stars. X-rays are the one spectral region where low-mass main sequence companions can be detected, since at other wavelengths the supergiants outshine dwarfs.

A useful comparison to the fraction of Cepheid plus low-mass systems is the determination of low-mass companions of B and early A stars since these are the stars that evolve into Cepheids. A Chandra observation of the cluster Trumpler 16 was used to identify X-ray sources among these stars (Evans, et al. 2011). Since B and early A stars do not typically produce X-rays, it was assumed that low-mass companions were the X-ray producers. They concluded that 39% of these late B stars have a low-mass companion. Two small points are of note in this comparison. Cepheids are slightly older than Tr 16 B stars which are $\simeq 3$ Myr. Also this fraction in Tr 16 includes companions at all separations, where Cepheid binaries with separations smaller than 1 au have been removed due to RLOF during the red giant phase. However the Tr 16 results are a good comparison to the Cepheid results in this study.

A second aspect of the present study is that Cepheid upper atmospheres have several properties including X-rays which may bear on outstanding questions. Cepheids frequently have excess infrared (IR) emission from circumstellar envelopes (CSEs) summarized by Gallenne, et al (2021), and Hocde, et al. (2020a,b, 2021). This effect needs to be quantified to allow precise distance determinations using the Cepheid Leavitt (Period-Luminosity) law in the IR. In addition, the CSEs are related to the long-standing question of possible mass loss in Cepheids. X-ray flux controlled by the pulsation cycle may be a driver of CSEs, and hence a clue to understanding both mass loss and the IR Leavitt Law.

This study begins with new Chandra observations of two Cepheids (*l* Car and Polaris) near maximum radius to determine whether they show the flux increase observed in δ Cep. These new data have then been combined with archival data to investigate the occurrence of young low-mass X-ray active companions.

l Car is an important Cepheid because it is bright and also has a long pulsation period (35^d). Long period Cepheids are vital for determining distances to external galaxies. Like many long period Cepheids, it has modest variation in some of its parameters such as its period. This was explored in detail with a combination of radial velocities and interferometry by Anderson, et al. (2016).

Polaris is the nearest and brightest Cepheid. An ongoing program is measuring its mass from its astrometric orbit (Evans, et al. 2018). The distance to Polaris has been controversial recently. However, the Gaia EDR3 parallax to the resolved companion Polaris B now seems to provide a reliable value of 137 pc (Evans et al. 2018). Polaris has been

observed four times in X-rays, once by Chandra (Evans, et al. 2010) and three times by XMM-Newton (Engle 2015). All four observations have a reasonably constant X-ray luminosity $\simeq \log L_X = 28.9$ ergs s^{-1} . However, none of the observations have been made at the “phase of interest” (maximum radius) for comparison with the X-ray burst of δ Cep. To add to the information about the upper atmosphere, HST COS spectra provide chromospheric emission lines which have been analyzed by Engle (2015). Polaris also has a radius and CSE measured by interferometry (Merand, et al. 2006).

In this paper, subsequent sections discuss observations of l Car and Polaris at maximum radius to search for increased X-ray flux at this phase, and the relation of X-ray observations to the pulsation cycle. The sample of X-ray observations of Cepheids is assembled from the new observations, upper limits from the survey investigating resolved companions, and observations where the Cepheids and low-mass companions were detected. This combined sample is compared with X-rays from main sequence stars. Finally the discussion includes the fraction of Cepheids in binary and multiple systems and the implications for star formation of these intermediate mass stars with small mass ratios.

2. OBSERVATION AND DATA ANALYSIS

In order to investigate further the X-ray flux from Cepheids, observations of two stars (l Car and Polaris) were made with Chandra. The observations were timed exposures with the ACIS-I instrument, and are listed in Table 1. Reductions were done with the standard *CIAO* software package.¹

l Car

The long period Cepheid l Car is known to have period fluctuations like other long period Cepheids (Anderson, et al, 2016a; Anderson 2016b). The phases of the observations were computed from the period summary in Neilson, et al. (2016), including the changing period. The time of observation was selected based on the relation between maximum radius and the burst of X-rays in δ Cep, where the X-ray burst occurs approximately 0.1 in phase after maximum radius. The phase of maximum radius has been measured in 3 successive cycles by Anderson, et al. (2016a), providing a recent determination of the time of maximum radius. The phase of R_{max} is 0.40, leading to a requested phase of the X-ray observation of 0.50. The phases of observations are listed in Table 1. The observation had to be broken into two parts for scheduling reasons, as listed in Table 1. Note that for a period of 35^d , the duration of the longer exposure covers only 0.02 in phase,

No source was detected at the position of the Cepheid l Car. The upper limit to the flux was estimated as follows, using $E(B-V) = 0.17$ mag (Ferne, et al. 1995), the conversion to N_H from Seward (2000; $N_H/E(B-V) = 5.9 \times 10^{21}$ atoms cm^{-2} mag^{-1}) and a distance of 506 pc (Evans et al 2016a). Distances for Cepheids (except Polaris) are taken from Evans, et al., (2016a) based on the HST FGS scale of Benedict, et al (2007). Less than 1 count was found for l Car in 58.3 ksec. Using PIMMS, this provides an unabsorbed flux of 5.88×10^{-16} ergs s^{-1} cm^{-2} . At the distance of the Cepheid, this corresponds to a luminosity L_X of 1.75×10^{28} ergs s^{-1} ($\log L_x = 28.26$). The luminosity upper limit for the short exposure is $\log L_x = 28.70$ and for the combined exposure $\log L_x = 28.11$. Uncertainties on the upper limits are based on the variance of the background. For l Car, the exposure time (corrected to 44 ksec of good time intervals) corresponds to a 9% uncertainty, or a difference of 0.04 in $\log L_X$.

Polaris

For Polaris, similarly, the observation was requested to coincide with the predicted time of X-ray increase shortly after maximum radius. Phases of observation were computed from the recent ephemeris (Engle 2015): 2,455,909.910 + 3.972433 E. The phase range covered by the observation is 0.48 to 0.69.

A source was detected at the position of Polaris. A flux was determined by fitting the spectrum with a MEKAL model in *CIAO* with $E(B-V) = 0.00$ and a fixed temperature of 0.56 keV, typical of a young star. MEKAL models were used for consistency with data from Engle (2015), however tests with newer APEC models agreed to 10%. The resulting flux is 2.08×10^{-14} ergs s^{-1} cm^{-2} . The distance used to determine the luminosity is 137 pc from the Gaia EDR3 distance to the resolved companion Polaris B. Because of the length of the exposure, the luminosity was computed for two halves, $\log L_X$ 28.83 and 28.71 [ergs s^{-1}]. The details are listed in Table 1.

¹ <https://cxc.cfa.harvard.edu/ciao/>

Table 1. Chandra Observations

OBSID	Instrument	Exp ksec	JD mid	Phase	D pc	log L_X [ergs s ⁻¹]
<i>l</i> Car						
20149	ACIS-I	58.27	2,458,388.9999	0.53	506	<28.26
21858	ACIS-I	20.8	2,458,494.8437	0.51		<28.70
Polaris						
18928	ACIS-I	69.16	2,457,942.1482	0.48-0.59	137	28.83
				0.59-0.69		28.71

3. THE PULSATION CYCLE

The interest in X-ray production in Cepheids is enhanced by its relation to other parameters of the pulsation cycle. In the case of δ Cep (Engle, et al. 2017), a brief X-ray burst was seen shortly after *maximum* radius. This is in contrast to ultraviolet chromospheric lines which go into emission after *minimum* radius.

***l* Car:** The relation of the X-ray observations in Table 1 to other pulsation parameters is shown in Fig. 1, adapted from Neilson, et al. (2016). Successive panels show emission lines from HST COS, spectra, and from the International Ultraviolet Explorer satellite (IUE) spectra, upper limits from Chandra (Table 1) and XMM-Newton observations, V band photometry (Neilson, et al., 2016) and radial velocities (Taylor, et al 1997).

Polaris: The relation of the X-ray observations of Polaris to the pulsation cycle variables is shown in Fig. 2. Successive panels show N V and Si IV emission lines from HST COS spectra (Engle 2015), X-ray observations, V band photometry (Engle 2015 plus some additional data from the same system), and radial velocities (Anderson 2019). Four previous observations with XMM-Newton and Chandra are listed in Engle (2015).

4. X-RAY OBSERVATIONS OF CEPHEIDS

In addition to the observations of *l* Car and Polaris, X-ray observations have been made of a number of Cepheids. δ Cep, β Dor, *l* Car, and SU Cas are discussed in Engle (2015). Observations of V473 Lyr and η Aql are discussed in Evans, et al. (2020b) and Evans, et al. (2021) respectively. Finally, a survey was made with XMM-Newton of possible resolved companions (Evans et al. 2016b). In this section we discuss these observations in three subsections: upper limits in cases where the Cepheid was not detected (Table 2), cases where the Cepheid was detected (Table 3), and cases where a low-mass companion was detected (Table 4).

4.1. Upper Limits for Cepheids and Close Companions

A series of observations was conducted with XMM-Newton of Cepheids with possible resolved low mass companions (Evans, et al. 2016b). The resolved companion candidates are separated from the Cepheids typically by $10''$, hence these observations also provide an X-ray observation of the Cepheid and any possible close companion as well. For the resolved companions, because low mass stars at the age of Cepheids are X-ray active, they can be distinguished from old line-of-sight field stars in X-ray observations. The companion candidates in the XMM-Newton survey were identified in an HST Wide Field Camera 3 (WFC3) snapshot survey. The exposure time was set to detect a late spectral type companion (see Section 4.4). Because young low mass main sequence stars are more X-ray active than supergiant Cepheids, in general the observations of the Cepheids themselves are upper limits. They are summarized in Table 2. Columns in Table 2 list the star, the satellite used, the epoch and period used to compute the phase where they are not provided in another source, the reference for the period, the JD of mid exposure where it is not listed elsewhere, the pulsation phase of the observation, the distance D from Evans, et al (2016a) and the log of the X-ray luminosity of the upper limit. The distances are on the Benedict, et al. (2007) scale. Where the observations covered a significant range of phases, the range is shown. For most observations, the exposure time only covered ± 0.03 in phase. The upper limits are based on a 3σ detection since the positions of the sources are known, as discussed in Evans, et al (2016b). Uncertainties for the upper limits were estimated from the standard deviation of the local

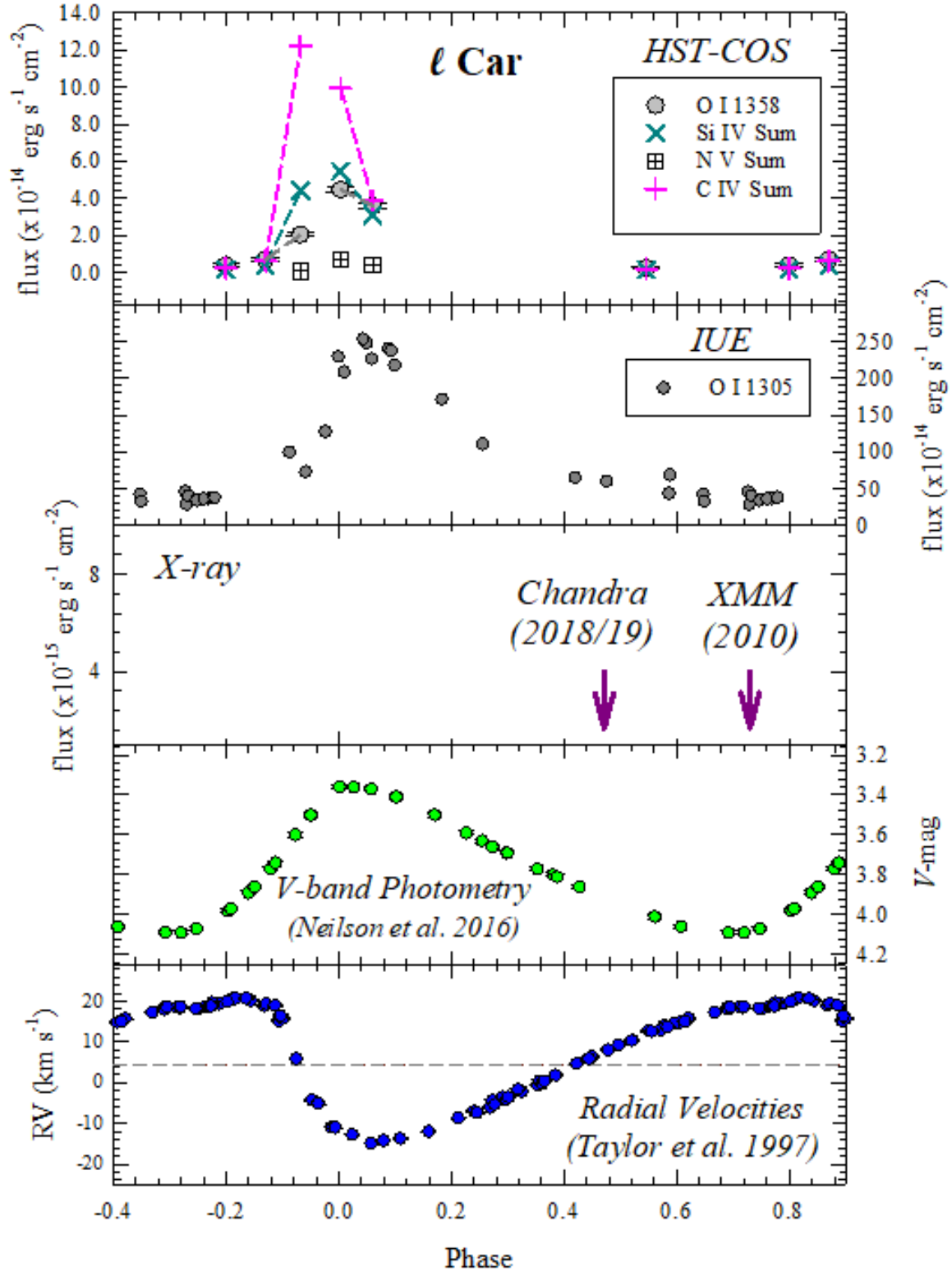


Figure 1. Multiwavelength observations of l Car as a function of pulsation phase. Panels top to bottom show emission lines from HST COS spectra, emission lines from IUE spectra, X-ray observations, V photometry, and radial velocities as discussed in the text.

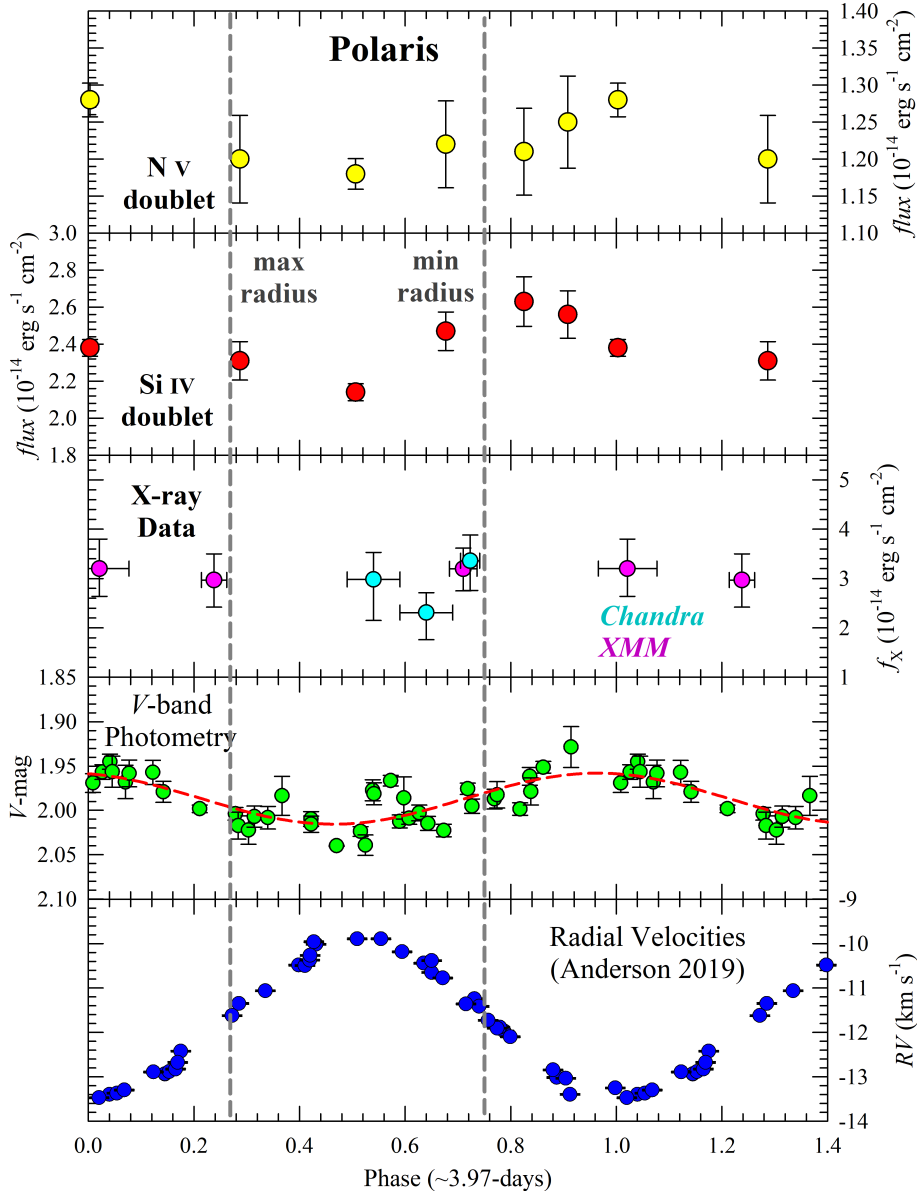


Figure 2. Multiwavelength observations of Polaris as a function of pulsation phase. Panels top to bottom show N V emission lines and Si IV emission lines from HST COS spectra, X-ray observations, V photometry, and radial velocities as discussed in the text. The error bars on the X-ray phases indicate the time period covered by the observations. The Chandra observation in Table 1 has been broken into 2 parts.

background. As a typical example, V440 Per has an exposure time of 21 ksec and an uncertainty on the upper limit of 9%, corresponding to 0.04 in $\log L_X$.

The upper limits to Cepheid X-rays are plotted in Fig. 3.

In addition, upper limits to two Cepheids (SU Cas and l Car) were reported by Engle (2015) from XMM-Newton observations which are listed in Table 2. Neither was detected. For the short period Cepheid SU Cas ($P = 1.95^d$; the upper limit $\log L_X = 29.46$ ergs s^{-1} was estimated using exposure times and background rates, and a distance $D = 376$ pc. For l Car the upper limit was estimated using a distance 506 pc to be $\log L_X = 29.62$ ergs s^{-1} .

η Aql was also observed by XMM-Newton (Evans, et al. 2021) but not detected (Table 2), providing an upper limit.

Table 2. X-ray Upper Limits of Cepheids

	Sat	T_0 -2,400,000	P d	Ref	JD mid -2,400,000	Phase	D pc	$\log L_X$ ergs s^{-1}
η Aql	XMM	55856.689	7.177025	1	58616.02	0.41-0.53	273	< 29.23
l Car	Chan	37751.5	35.535	2	58389.00	0.55	506	< 28.26
l Car	Chan			2	58494.84	0.52	506	< 28.70
l Car	XMM			3	55232.31	0.76	506	< 29.62
SU Cas	XMM	55199.614	1.949330	3	55236.27	0.64-0.98	376	< 29.46
V737 Cen	XMM	55118.3272	7.0659	4	56684.28	0.62	848	< 29.40
S Cru	XMM	34973.495	4.689970	5	56525.48	0.34	724	< 29.60
X Cyg	XMM	43830.251	16.385692	6	56408.79	0.65	981	< 29.89
R Mus	XMM	26496.033	7.510159	5	56338.66	0.63	844	< 29.48
S Nor	XMM	44018.884	9.754244	5	57095.07	0.56	910	< 29.44
Y Oph	XMM	39853.173	17.126908	5	56182.84	0.45	510	< 29.29
V440 Per	XMM	44551.137	7.572498	6	56538.55	0.02	791	< 29.17
U Sgr	XMM	30117.955	6.745229	5	54020.65	0.64	617	< 29.05
Y Sgr	XMM	40762.329	5.773380	5	56564.79	0.12	505	< 29.25

Period source: 1. Evans, et al. 2021; 2. Table 1; 3. Engle, S. 2015; 4. Usenko, I, et al. 2013; 5. Szabados, L. 1989; 6. Szabados, L. 1991;

4.2. Detections of Cepheids

For the Cepheids δ Cep, β Dor, and Polaris the Cepheid itself was detected (Engle 2015). The observations are listed in Table 3 and are shown in Fig. 3.

There is some evidence for a low mass companion to δ Cep from radial velocities (Anderson et al. 2015) interferometry (Gallenne, et al. 2016) and Gaia (Kervella, et al. 2019b). While this is possible, Fig. 3 shows that the X-ray level is lower than any main sequence star hotter than spectral type M.

In the 10^d Cepheid β Dor a variation in luminosity is seen, with the largest value at about the same level as the maximum luminosity of δ Cep. The 10^d Cepheids fall in the Hertzsprung progression of light curves where the pulsation amplitude is decreased by the coincidence of the primary and secondary humps. This may distort the phase of maximum light which is the standard ephemeris fiducial. We have determined the phase of the X-ray increase in β Dor as follows. For δ Cep (Fig. 1 in Engle, et al. 2017) both the phases when the pulsation wave passes through the photosphere at minimum radius and the phase of X-ray maximum shortly after maximum radius are well determined from FUV lines and X-ray fluxes respectively. The X-ray flux maximum occurs 0.66 phase after the FUV flux maximum. Similarly, the phase of FUV maximum (minimum radius) of the photospheric pulsation wave is well determined for β Dor. If we match the phases of UV maximum in δ Cep and β Dor (by adding 0.17 to the phase of UV maximum in β Dor), the phase of X-ray maximum becomes 0.42, as shown in Fig. 3 very similar to the phase of δ Cep. This phase adjustment is included in the β Dor phases in Table 3.

Table 3. X-ray Detections of Cepheids

	Sat	Ref	Phase	D pc	log L _X ergs s ⁻¹
Polaris	XMM	1	0.21-0.26	137	28.82
Polaris	XMM	1	0.68-0.74	137	28.86
Polaris	XMM	1	0.97-0.08	137	28.90
Polaris	Chan	1	0.71-0.73	137	28.88
Polaris	Chan	2	0.48-0.59	137	28.83
		2	0.59-0.69	137	28.71
δ Cep	XMM	3	0.33-0.39	255	28.60
	XMM	3	0.43-0.48	255	29.17
	XMM	3	0.48-0.54	255	28.90
	XMM	3	0.54-0.59	255	28.66
	XMM	3	0.05-0.12	255	28.67
	XMM	3	0.84-0.96	255	28.53
	XMM	3	0.96-0.08	255	28.53
	XMM	3	0.58-0.68	255	28.46
	XMM	3	0.68-0.78	255	28.66
	Chan	3	0.48-0.52	255	29.16
	Chan	3	0.52-0.56	255	28.95
β Dor	XMM	1	0.58-0.62*	335	29.24
β Dor	XMM	1	0.64-0.68*	335	29.11
β Dor	XMM	1	0.69-0.73*	335	28.94

Sources: 1. Engle 2015; 2. Table 1; 3. Engle, et al. 2017

* Phases adjusted; see text

4.3. Detections of Cepheid Companions

Table 4. X-ray Detections Cepheid Companions

	Sat	T ₀ -2,400,000	P ^d	Ref P	JD mid -2,400,000	phase	D pc	log L _X ergs s ⁻¹
V473Lyr	XMM	—*	1.490813	1	56557.96	0.47	553	29.88
	XMM			1	58560.00	0.42-0.73		30.07
S Mus	XMM	40299.163	9.659875	2	56298.26	0.24	789	30.46
W Sgr	XMM	43374.622	7.594904	2	57637.64	0.97	409	29.78
	XMM				57659.39	.836		
V659 Cen	XMM	52358.9089	5.62316689	3	56543.46	0.14	753	29.51
R Cru	XMM	55172.5100	5.825701	4	56662.46	0.73	829	29.80

Table 4 continued on next page

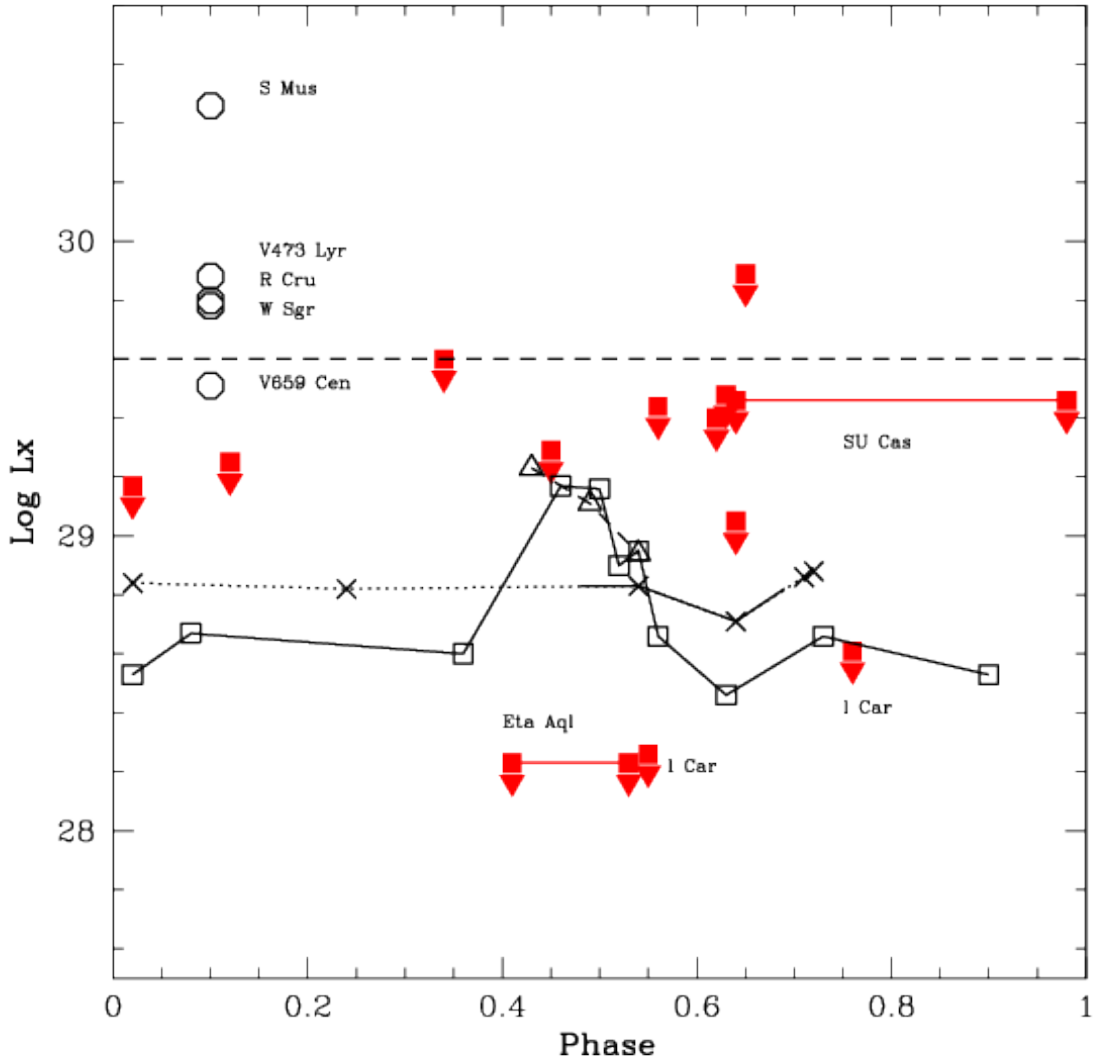


Figure 3. X-ray observations of Cepheids. Upper limits from non-detections in Table 2 are filled red down arrows; detections of Cepheids in Table 3 are: connected open squares: δ Cep, connected x's: Polaris; connected triangles: β Dor. The solid portion of the Polaris data line shows the phase range of the new observation in Table 1. For η Aql and SU Cas upper limits are indicated and the lines show the phase range covered. The mean $\log L_X = 29.6$. Circles in the upper left (labeled) are systems where the low-mass companion dominates the X-rays (Table 4). Luminosity is in ergs s^{-1} .

Table 4 (continued)

Sat	T_0	P	Ref	JD mid	phase	D	$\log L_X$
	-2,400,000	^d	P	-2,400,000		pc	ergs s^{-1}

Sources: 1. Evans et al. 2020b; 2. Szabados 1989; 3. Berdnikov et al. 2000; 4. Usenko et al. 2014

* The phase for V473 Lyr very variable.

In some cases X-ray observations identified low mass companions of Cepheids. Each of those will be discussed in this section. They are summarized in Table 4 and Fig. 3.

V473 Lyr: This is a unique Cepheid with a variable amplitude, perhaps similar to the Blazhko effect in RR Lyrae

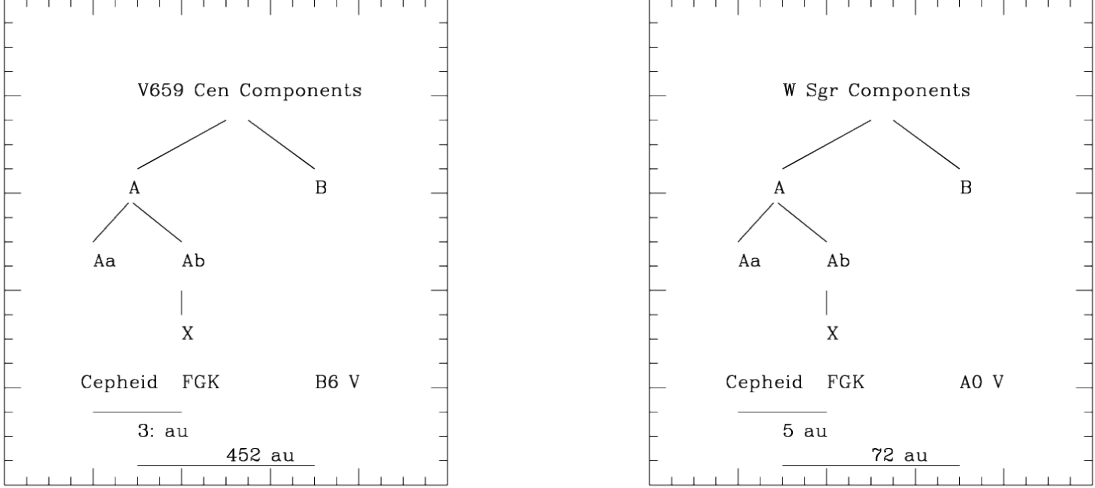


Figure 4. a. (left) The V659 Cen system. The diagram of the components indicates the Cepheid and the spectral types of the close and distant binary. Star Ab is a low-mass star (FGK) which produces the X-rays. The separations of the systems in au is indicated at the bottom. (The separation in the Aa–Ab binary is only an estimate.) b. (right) The W Sgr system, with the same notation as a.

stars. A recent XMM-Newton observation (Evans, et al. 2020b) was made to follow up a possible X-ray burst. However, the X-ray flux remained constant for a third of the pulsation cycle, making a low mass companion the most likely interpretation. Limits from radial velocities and Gaia proper motions are consistent with a companion at a separation between 30 and 300 AU.

V659 Cen: The Cepheid is in a multiple system and its components are only identified using a number of approaches. A resolved companion at $0.6''$ (452 AU) was found in a HST WFC3 survey of Cepheids (Evans et al. 2013). The system was found to be an X-ray source in the XMM-Newton survey of possible resolved companions (Evans, et al 2016b) with $\log L_X = 29.51 \text{ ergs s}^{-1}$ at a pulsation phase of 0.14. In the summary discussion of the HST WFC3 survey, Evans et al. (2020a), found that systems with a resolved companion also have an inner spectroscopic binary. Evidence for an inner binary in the V659 Cen system discussed there include orbital motion in velocities and possible orbital motion in Hipparcos proper motions. Can we identify the source of the X-rays in the triple system? In comparison with Cepheids which have themselves been detected in X-rays (Table 3), V659 Cen has a much larger X-ray flux, particularly at the phase of the observation. V659 Cen B, the hottest star has a spectral type of B6 V from the ultraviolet spectrum (Evans et al 2020a). The same study discusses an HST STIS ultraviolet spectrum oriented to resolve the Cepheid and the $0.6''$ companion, which shows that the hottest star in the system is the resolved companion V659 Cen B. Could the X-rays be produced by that star? X-rays are produced by O and early B stars (Berghoefler et al. 1997; Naze, et al. 2011). However the dividing line for X-ray producers is approximately B3 V. V659 Cen B is cooler than that and unlikely to produce X-rays. The spectroscopic binary companion V659 Cen Ab is a lower mass star, and hence should be able to produce X-rays, and, indeed the X-ray flux is reasonable for an F, G, or K star. The components are summarized in Fig 4a.

R Cru X-ray flux from the R Cru system was discovered by Evans, et al (2016b) in an XMM-Newton survey of possible resolved companions. The HST observations showed two possible companions as sources of the X-rays, one at $1.9''$ and a closer spectroscopic binary. A shallower Chandra exposure localized the X-rays to the spectroscopic binary companion (Evans, et al 2020a). (Removal of the $1.9''$ companion also removes the most discordant point in the CMD of companions in Fig. 6 in Evans, et al. [2020a]). In addition, there is a star at $7.7''$ (Evans, et al. 2020a; Kervella, et al. 2019b). It was considered a likely companion from Gaia DR2 data. However, in the EDR3 data, both the parallax and the proper motion do not match those of the Cepheid as closely and they are less likely to be physically related. The system thus contains a Cepheid R Cru Aa, and the likely spectroscopic binary companion R Cru Ab. (Evans, et al 2020a). The X-ray luminosity in Table 4 is from the deeper XMM-Newton observation,

S Mus X-rays were similarly discovered in the S Mus system in the XMM-Newton observation by Evans, et al (2016b), which was followed by a Chandra observation to localize the X-rays (Evans, et al 2020a). In this case, the X-rays come from a spectroscopic binary with a period of 505 days made up of the Cepheid and a B3 V companion.

A companion this hot can produce X-rays through wind shocks, so the most likely interpretation is that the hot companion is responsible for the X-rays. S Mus is thus the one Cepheid which is not an X-ray test for a low mass companion. The X-ray luminosity in Table 4 is from the XMM-Newton observation.

W Sgr X-ray flux was found at the location of the Cepheid by XMM-Newton, listed in the source catalog 4XMM-DR11². There are in fact 2 XMM-Newton observations of W Sgr. In the second, the star is at the border of a chip, hence the flux is less precise. The stacked observation has a flux of $3.0 \pm 0.4 \times 10^{-14}$ ergs s⁻¹ cm⁻² in 0.2-12 keV. This is $\log L_X = 29.78$ at 409 pc.

W Sgr is part of a triple system (Evans, Massa, and Proffitt 2009). The hottest companion to the Cepheid, W Sgr B, has spectral type A0 V (Evans, et al, 2013) and was resolved from the spectroscopic binary in an HST STIS spectrum (Evans, Massa, and Proffitt 2009) at a projected distance of 72 AU. The spectroscopic binary Aa + Ab has separation of 5.0 AU (Benedict, et al. 2007). Only an upper limit could be obtained for the mass and spectral type of the companion from the STIS spectrum ($<1.4 M M_\odot$ and later than F5 V). This is consistent with the X-ray luminosity. Components are summarized in Fig 4b.

4.4. X-rays from Main Sequence Stars

Studies of activity in main sequence stars have been a very important area of X-ray study. The X-ray luminosities in the sequence of open clusters of different ages are summarized, for instance, in Prebisch and Feigelson (2005). The age of a stars found in the instability strip depends on their mass and hence their pulsation period. A typical age is 50 Myr as discussed by Bono, et al. (2005). This is between the ages of the Orion Nebula Cluster and the Pleiades, with the α Per cluster being a good representation of stars of this age. Its age is estimated to be 50 Myr (Meynet et al. 1993) to 90 Myr (Stauffer, et al. 1999). A study was made by Randich, et al. (1996) of ROSAT observations of the full cluster found that at a depth of $\log L_X$ to be 29.5 ergs s⁻¹, 76% and 79% of G and K stars were detected. Even for F stars 75% were detected although early F stars are not strong X-ray producers. A more recent study of a deep XMM-Newton observation of the α Per cluster is presented by Pillitteri, et. al. (2013). They find a mean X-ray luminosity $\log L_X$ to be 29.63 ergs s⁻¹ for F main sequence stars, 29.74 ergs s⁻¹ for G dwarfs, and 29.56 ergs s⁻¹ for K dwarfs. M dwarfs are fainter, and are not expected to be detected in the present study. A line is included at 29.6 ergs s⁻¹ on Fig 3 to indicate the mean level of F, G, and K stars. There is, of course, a range of X-ray luminosities for any mass or spectral type. This is partly because of variation of rotation velocity between stars. In addition, cool stars have activity cycles. However, even at a depth of $\log L_X$ 29.5, Randich, et al. find they detect three quarters of F, G, and K stars or better.

5. LOW-MASS COMPANIONS OF CEPHEIDS

A sample of 20 Cepheids observed in X-rays has been assembled from observations made for a variety of purposes. The X-ray luminosity level has been established for quiescent phases from δ Cep and Polaris at $\log L_X \simeq 28.7$ ergs s⁻¹. On the other hand, deeper exposures for *l* Car and η Aql have not detected the Cepheid at $\log L_X$ 28.2 ergs s⁻¹.

For the Cepheids W Sgr, V473 Lyr, V659 Cen, and R Cru a young low mass companion dominates the X-ray range. For S Mus the X-ray flux is most likely produced by an early B hot companion, which reduces the sample to 19 Cepheids to look for low mass companions. For the remaining 15 Cepheids, the upper limits indicate that there is *not* a low mass companion. Thus, only 21% of the Cepheids clearly have a low-mass companion. This fraction would be increased slightly if 2 stars with upper limits above or on the dividing line were removed from the sample. The sample has some limitations. Systems with periods shorter than a year are not present in Cepheid samples because they would have disappeared due to RLOF, particularly at the tip of the red giant branch. The X-ray exposure depth was set to detect F, G, and K main sequence stars at the age of the Cepheids. Thus M companions would not have been detected. In X-ray studies of main sequence stars at this age, three quarters of F, G, and K companions would have been detected at this exposure depth. This correction would raise the fraction of systems with low-mass companions to $28_{-9}^{+13}\%$ (errors from binomial statistics). This is clearly much lower than a random selection of companions from the IMF (Chabrier 2003; Moe and Di Stefano 2017), at least for systems with separations greater than about 1 au.

6. DISCUSSION

6.1. Binary/Multiple Fraction of Cepheids

² <http://xmm-catalog.irap.omp.eu/sources>

All methods of identifying Cepheid companions have some limitations. The X-ray observations in the current paper do not detect companions of spectral types earlier than F or later than K. However they identify companions at any separation. Similar properties are true for ultraviolet (UV) surveys: they identify companions earlier than mid-A at any separation (Evans, et al. 2013). Radial velocities (Evans et al. 2015) and Gaia proper motions (Kervella, et al. 2019a), on the other hand, are sensitive to a wider range of spectral types but detect short period small separation systems, but not longer period systems. Velocity studies are also much more sensitive for sharp-lined stars such as Cepheids than for broad-lined hot stars.

Ultimately, results for X-ray studies and ultraviolet studies of Cepheids need to be combined into the binary/multiple star fraction. The X-ray fraction (28%) and the UV fraction (21%; Evans 1992) are comprehensive for the companion spectral types they cover. However, Cepheids like other intermediate and massive stars are frequently found in systems with more than two members, and thus results from these two “detection wavelength” approaches would sometimes overlap. We can make a rough estimate of this from this study, in that of the 4 Cepheids with a late type companion two (V659 Cen and W Sgr) were already known to be in multiple systems from UV studies. That is, only half the low-mass companions (14%) are new systems in the total, resulting in 35% of Cepheids in binary or multiple systems from the combined X-ray and UV studies. This is, of course, a lower limit since it does not represent all companion spectral types. We can further make rough estimates of the companions which are left out of these two spectral type regions. The UV spectra identify all massive companions but have serious incompleteness starting at mid-A spectral types, corresponding to a mass of approximately $1.9 M_{\odot}$. Table 5 summarizes information about these spectra type regions (bins). The top row lists the spectral types of the hot and cool boundaries of the UV and X-ray surveys. Corresponding masses are listed in the next line taken from Drilling and Landolt (2000). Below the masses, the entries list information for the four bins. The mass ratio is shown for the mass range in the bin. The bottom line shows for percentage of companions measured in bins 1 and 3. The mass ratios in line 3 are quite similar for the X-ray and UV regions and also for the regions not covered. Following the results from the IMF (Chabrier 2003), the region in bin 2 not sampled in X-ray or UV is expected to have somewhat fewer stars than the sampled regions and hence fewer binary companions. Thus the missing region in bin 2 would probably not double either the fraction in bins 1 and 3, or the combined fraction (35%), but it would add significantly. Similarly, the missing M stars in bin 4 would substantially increase the fraction. However, we have shown here that the fraction of cool companions in binary systems is less than predicted by a field IMF. In sum, the binary fractions in the bins 1, 2, and 3 are 21%, <21%, and 28%. A simple total is <70%. It would be reduced somewhat by an overlap of UV and X-ray companions in multiple systems. However, it would be increased by a substantial but unknown fraction of M stars in bin 4.

Table 5. Mass/Spectral Type Regions for Companion Detection

Bin	Sp Ty UV	Sp Ty UV	Sp Ty X	Sp Ty X	
	Hot	Cool	Hot	Cool	
	1	2	3	4	
Spectral Type	B5	A5	F5	M0	M5
Mass M_{\odot}	5.9	1.9	1.4	0.51	0.21
Mass Ratio	3.1	1.4	2.8	2.4	
Companion %	21	–	28	–	

The second binary/multiple detection technique is through orbital motion, either with radial velocities or with proper motions. Evans et al. (2015) examine orbital motions for the 40 brightest Cepheids N of -20° from two CORAVEL studies. They find a binary fraction of 29% with orbital periods between 1 and 20 years where the sample is most complete. This rises to 35% for all periods greater than 1 year for the nearest 40 stars. There is serious incompleteness for long orbital periods and low mass ratios. Since from this X-ray study, companions F5 V or cooler are likely to be at least half the binary fraction, the incompleteness rises substantially. Kervella, et al. (2019a) have compared Gaia DR2 proper motions with those from Hipparcos to identify deviations resulting from orbital motion (proper motion anomalies). Using their criterion for a detection of the ratio of proper motion difference to signal to noise of 3, for the

nearest 100 Cepheids, the binary fraction is 32%. This fraction doubles adding in binaries identified by other means, bringing it close to the estimate of 70% above.

Wider companions in orbits which would not be identified either from velocities or proper motions also exist. The challenge here is that as larger separations from the Cepheid are searched, a field star is more likely to be included in the list of companion candidates. This was tested with X-ray observations of a subset of possible resolved companions (Evans, et al. 2016b). No companion candidates with separations $>5''$ or 4000 au were confirmed to be physical companions. There are six systems with wider companions or possible companions in the HST survey (Evans, et al. 2020a), but most have a hot companion or are in spectroscopic binary systems, so they are already counted and do not add to the list of binary or multiple systems. Gaia DR2 and EDR3 parallaxes and proper motions have also been used to investigate companions at wider separations (Kervella, et al. 2019b; Breuval 2021). This is a very promising approach, but so far for the Cepheids within about 1 kpc, the companion candidates all have sizable errors in EDR3 parallaxes.

The most important feature in comparing the Cepheid binary fraction with that of B stars from which Cepheids evolved is RLOF for short period B binaries. The effects are particularly striking in O stars (Sana, et al. 2012). Moe and Di Stefano (2017) find that only 75% of mid-B stars will evolve into Cepheids. This means our fraction of Cepheids with low-mass companions (28%; Table 5) corresponds to a fraction of 37% of B stars.

The fraction of low-mass companions of Cepheids can be compared with that of “late B” stars in Tr 16 (39%) from a similar X-ray technique (Evans, et al. 2011). This is very close to the Cepheid fraction (37%). The fraction in Tr 16 might be somewhat higher since the cluster is younger than the Cepheids, and hence low-mass stars are more X-ray active and more easily detected. Furthermore, the Cepheid sample is limited to binaries with periods longer than a year. However the similarity of the fractions indicates that in both the occurrence of low mass companions is lower than would be predicted by random sampling from a field IMF.

6.2. Implications for Star Formation

Unresolved companions to Cepheids provide a unique probe into the properties of intermediate mass binaries across intermediate separations, which helps to constrain binary formation models. The unresolved companions must be wider than $a > 1$ au to avoid RLOF with the Cepheid supergiant primaries, and must also reside within $a < 1000$ au; otherwise we would have resolved the companions in our previous HST imaging campaign (Evans et al. 2020a). Our detected X-ray companions span late-F/G/K dwarfs, corresponding to masses $M_{comp} = 0.5-1.4 M_{\odot}$. For a typical Cepheid primary mass of $M_{Cepheid} \approx 5 M_{\odot}$, the binaries correspond to mass ratios $q = M_{comp} / M_{Cepheid} = 0.10 - 0.28$. After correcting for incompleteness of FGK stars that do not produce a detectable X-ray flux as described above, we conclude that $28_{-9}^{+13}\%$ of Cepheids have companions across $a = 1 - 1000$ au and $q = 0.10 - 0.28$ (red data point in Fig. 5), where the uncertainties derive from binomial statistics. For a larger sample of 76 Cepheids, 16 exhibited a UV excess from unresolved B/early-A dwarfs spanning $M_{comp} = 1.9 - 5.9 M_{\odot}$ (Evans 1992). We thus find that $21\% \pm 5\%$ of Cepheids have companions across $a = 1 - 1000$ au and $q = 0.37 - 1.00$ (magenta data point in Fig. 5). We are incomplete to late-A/early-F dwarf companions, which span the narrow mass-ratio interval $q = 0.28 - 0.37$.

As shown in Fig. 5, companions to Cepheids are skewed toward smaller mass ratios. Given the measured occurrence rate of B/late-A companions to Cepheids via the UV excess method and assuming a uniform mass-ratio distribution (dotted line in Fig. 5), we would have expected only 6% of Cepheids to have late-F/G/K companions across $q = 0.10 - 0.28$. This prediction is discrepant with our empirical measurement of $28_{-9}^{+13}\%$ at the 2.7σ level. Conversely, if we instead assumed that binaries were drawn from random pairings of the IMF (dashed curve in Fig. 5), we would have expected 87% of Cepheids to have companions across $q = 0.10 - 0.28$, which is even more inconsistent with our measurement at the 4.5σ level. The true mass-ratio distribution is between these two slopes. By fitting a single power-law distribution $p_q \propto q^{\gamma}$, we measure $\gamma = -1.2 \pm 0.4$ across $q = 0.1 - 1.0$ (blue curve in Fig. 5).

Close companions ($a < 1$ au) to mid-B stars follow a uniform mass-ratio distribution, indicating they coevolved via shared accretion in a circumbinary disk, while wide companions ($a > 1000$ au) are weighted toward extremely small mass ratios, nearly consistent with random pairings drawn from the IMF, suggesting the components fragmented and subsequently accreted fairly independently (Abt et al. 1990; Kouwenhoven, et al. 2007; Kobulnicky and Fryer 2007; Moe and Di Stefano 2017). Across intermediate separations, both long-baseline interferometry (Rizzuto, et al. 2013) and decomposition of binaries from high-resolution spectra (Gullikson, et al. 2016) demonstrated that the mass-ratio distribution is skewed toward small mass ratios. However, these techniques are insensitive to companions below $q < 0.3$. Our survey yields the first robust census of low-mass companions to intermediate-mass stars across intermediate separations, confirming earlier indications that the mass-ratio distribution is skewed toward small mass ratios but nonetheless still top-heavy compared to random pairings drawn from the IMF. Thus both disk and core fragmentation

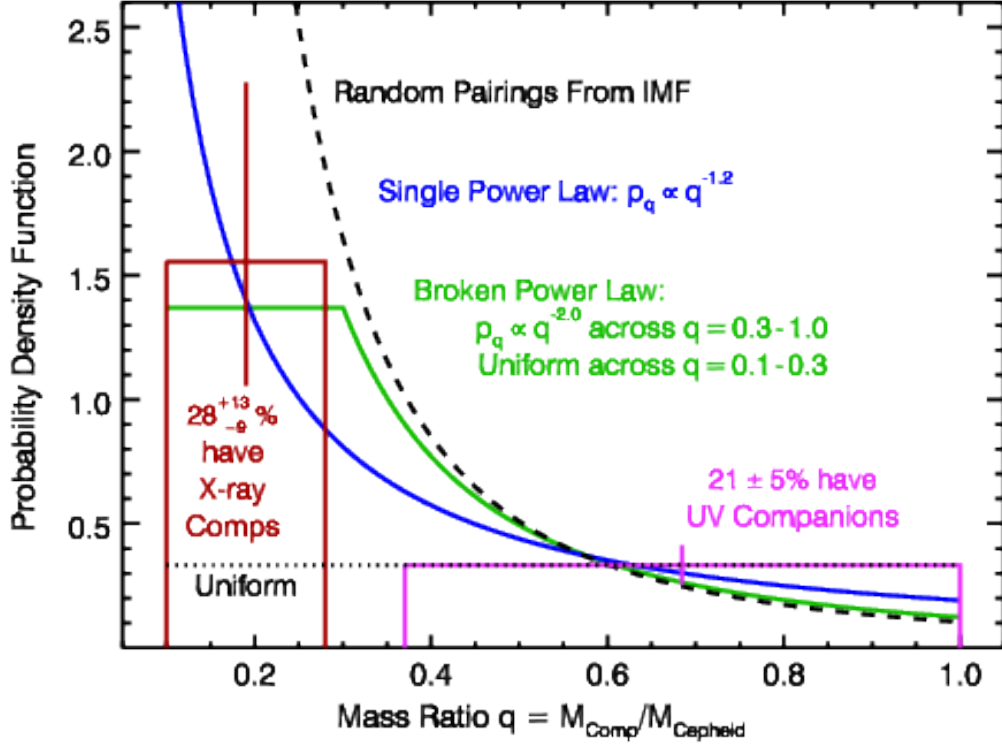


Figure 5. Our X-ray survey demonstrates that $28^{+13}_{-9}\%$ of Cepheids have unresolved late-F/G/K companions across $q = 0.10 - 0.28$ (red). Meanwhile, an earlier UV survey (Evans 1992) found that $21\% \pm 5\%$ of Cepheids have unresolved B/early-A companions across $q = 0.37 - 1.0$ (magenta). The measured mass-ratio distribution is inconsistent with both a uniform distribution (dotted) and random pairings of the IMF (dashed). We fit a power-law distribution with an intermediate slope of $\gamma = -1.2 \pm 0.4$ across $q = 0.1 - 1.0$ (blue). The data are also consistent with the segmented power-law model adopted in Moe & Di Stefano (2017; green). In total, we find that $57\% \pm 12\%$ of Cepheids have companions across $q = 0.1 - 1.0$ and $a = 1 - 1,000$ au.

and accretion lead to a mixed population of intermediate-period binaries.

Moe & Di Stefano (2017) adopted a segmented power-law mass-ratio distribution with the parameter $\gamma_{\text{large}q}$ describing the slope across large mass ratios $q = 0.3 - 1.0$ and $\gamma_{\text{small}q}$ across $q = 0.1 - 0.3$. They fitted both power-law slopes as a function of primary mass and orbital separation based on a combination of datasets, interpolating over the gaps in the observations. For intermediate-period companions to $5M_{\odot}$ primaries, they fitted $\gamma_{\text{large}q} = -2.0$ and $\gamma_{\text{small}q} = 0.0$ (green curve in Fig. 5). This distribution is significantly skewed toward small mass ratios, nearly consistent with random pairings of the IMF across $q = 0.3 - 1.0$, but then flattens to a uniform distribution below $q < 0.3$. Their broken power-law model is also consistent with our measurements.

We can now determine the overall unresolved binary fraction of Cepheids. By interpolating our best-fit power-law model across the mass ratio gap where both X-ray and UV methods are insensitive, we expect an additional 8% of Cepheids to have late-A/early-F companions across $q = 0.28 - 0.37$. Thus $57\% \pm 12\%$ of Cepheids have companions across $q = 0.1 - 1.0$ and $a = 1 - 1000$ au. This is consistent with expectations from mid-B binaries. Moe & Di Stefano (2017) estimated that 85% of $5M_{\odot}$ MS primaries have companions above $q > 0.1$, of which 70% have intermediate separations spanning $a = 1 - 1,000$ au. Hence, $0.85 \times 0.70 = 60\%$ of mid-B stars have companions across intermediate separations, nearly identical to our Cepheid result.

The X-ray studies here demonstrate that the fraction of F, G, and K companions is smaller than would be produced by random pairings of the IMF (Fig. 5). To complete the understanding of companion distribution, we need to know the form of the distribution of M star companions. A recent study of b Cen, a 6-10 M_{\odot} binary demonstrates that even a planet can exist around a massive star (Janson, et al. 2022), providing the need to hunt for even smaller objects. Observing a sample of M stars to explore the mass distribution would require very long exposures in X-rays. Kervella et al (2022) discuss the use of Gaia EDR3 proper motions and parallaxes to identify companions around stars within 100 pc through proper motion anomalies (PMa; orbital motion) and common proper motion pairs (CPM). This sample

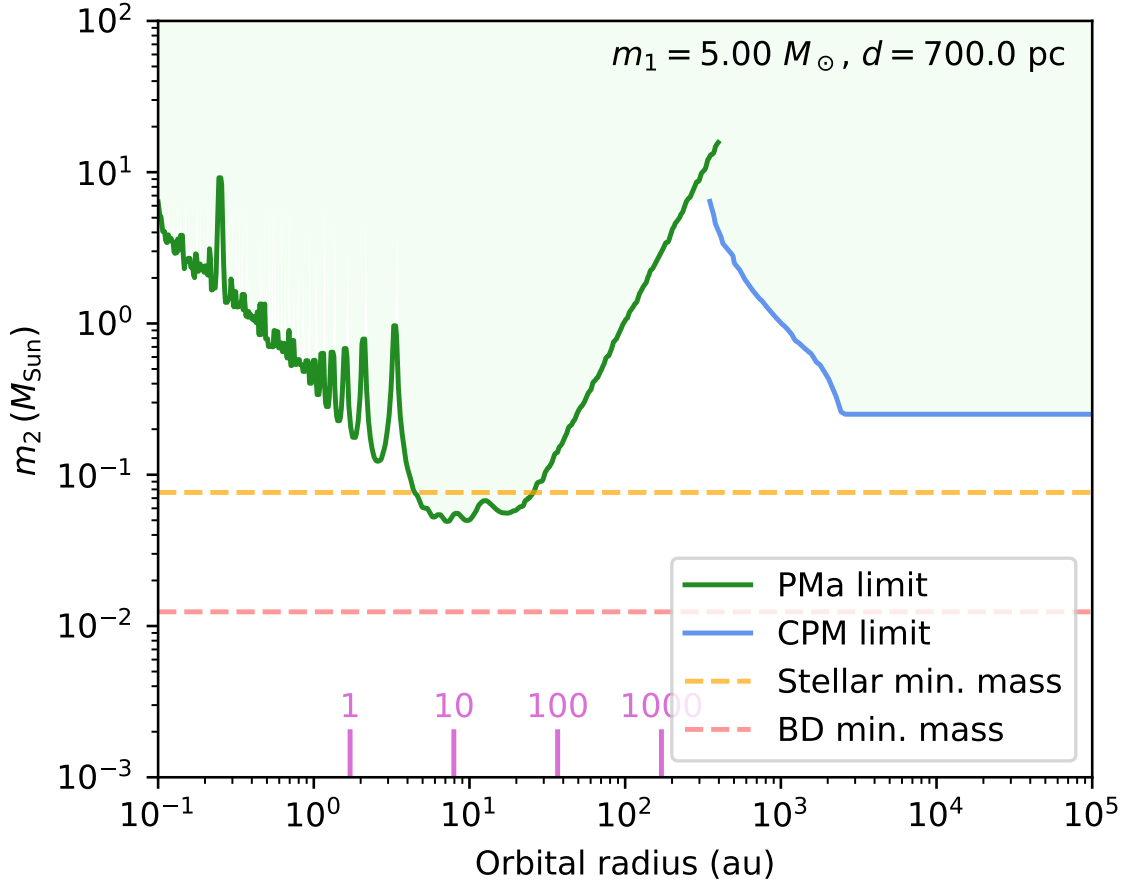


Figure 6. Companion Detection Sensitivity for Cepheids from Gaia EDR3. Sensitivity for companion mass is shown as a function of orbital radius and orbital period. Green line: limit from proper motion anomaly; blue line: limit for common proper motions; yellow dashed line: stellar mass limit; pink dashed line: brown dwarf limit; orbital period in years is shown by the pink lines on the x-axis. Cepheid parameters are $5.0 M_{\odot}$ and 700 pc, typical parameters in this study. The green region above the stellar limit indicates that stellar companions at the low-mass stellar limit will be detected for orbital periods between about 3 and 100 years.

includes relatively few massive stars, however they find that 45% of the sample have an indication of binarity and 7% have bound CPM candidates. They estimate that as many as 70% of Cepheid-mass stars could have PMA and CPM companions. Fig 6 shows the detection limits for a typical Cepheid in this study ($5M_{\odot}$ and 700 pc) in EDR3. Stars down to the low-mass limit should be detected for orbital periods between about 3 and 100 years. This limit will improve substantially in future Gaia releases, to approximately $4 \times$ better in DR4 (2024) and $13 \times$ better in DR5 (2027).

7. SUMMARY

In this section we summarize the main points of this study.

7.1. *l Car and Polaris*

As shown in Fig 3, *l Car* has an X-ray luminosity which is below the quiescent phases of δ Cep, and certainly below the X-ray burst at maximum radius in δ Cep. Because *l Car* has a longer period than δ Cep, we know it has a higher luminosity and mass, as well as reaching cooler minimum temperatures. Any of these could affect X-ray production, though it is not obvious that they would affect the convective surface to disrupt magnetic activity. While the observation was carefully timed for maximum radius, in a 35^d Cepheid, the 80 ksec exposure covers only 3% of the phase, so a phase-restricted burst could have been missed.

For Polaris, the X-ray luminosity is comparable to that of δ Cep in its quiescent phases. There is no indication of an X-ray burst even though much of the pulsation cycle has been covered. The observation discussed here alone covers a phase range of 0.48 to 0.69. Polaris pulsates in the first overtone mode and has a very low pulsation amplitude, which

could alter the X-ray–pulsation relation as compared with δ Cep (full amplitude and fundamental mode).

7.2. The Pulsation Cycle

A major motivation for the series of X-ray observations of Cepheids follows from the X-ray burst in δ Cep. Fig 3 shows that neither η Aql nor l Car share this behavior. As discussed above l Car differs from δ Cep in physical properties which might account for this. η Aql, on the other hand, has a period very similar to δ Cep, and hence, similar luminosity, mass, and temperature cycle. At this point, questions remain about the X-ray behavior of both stars. Polaris has no indication of a phase-related X-ray increase.

7.3. Low-Mass Companions

Chandra and XMM-Newton observations of a sample of 20 Cepheids finds that 28% have a low mass companion. The fraction of Cepheids with low-mass companions is very similar to that predicted from mid-B stars. This sample identifying F, G, and K spectral type companions can be combined with a previous survey in the UV which identifies B and early A companions. Using a Moe and Di Stefano segmented power law to fit the data, $57\% \pm 12\%$ have companions with the mass ratio $q > 0.1$ the separation $a > 1$ au. This is the first survey of intermediate mass stars that reaches to mass ratios this small. The mass ratio distribution falls between a uniform distribution and random pairings from IMF, that is between formation from shared accretion in a circumbinary disk and fragmentation and independently accreted components.

8. ACKNOWLEDGMENTS

This research is based on observations obtained with XMM–Newton, an ESA science mission with instruments and contributions directly funded by ESA Member States and the USA (NASA).

Support was provided to NRE by the Chandra X-ray Center NASA Contract NAS8-03060. The observations were associated with program 84051 with support for this work from NASA Grant 80NSSC20K0794. JJD was supported by NASA contract NAS8-03060 to the Chandra X-ray Center and thanks the Director, Pat Slane, for continuing advice and support. HMG was supported through grant HST-GO-15861.005-A from the STScI under NASA contract NAS5-26555. P.K. and L.B. acknowledge funding from the European Research Council (ERC) under the European Union’s Horizon 2020 research and innovation program (projects CepBin, grant agreement No 695099, and UniverScale, grant agreement No 951549). This work has made use of data from the European Space Agency (ESA) mission *Gaia* (<http://www.cosmos.esa.int/gaia>), processed by the *Gaia* Data Processing and Analysis Consortium (DPAC, <http://www.cosmos.esa.int/web/gaia/dpac/consortium>). Funding for the DPAC has been provided by national institutions, in particular the institutions participating in the *Gaia* Multilateral Agreement.

The SIMBAD database, and NASA’s Astrophysics Data System Bibliographic Services were used in the preparation of this paper.

REFERENCES

- Abt, Helmut A., Gomez, Ana E., Levy, Saul G. 1990, ApJS, 74, 551
- Anderson, R. I., Sahlmann, J., Holl, B., et al. 2015, ApJ, 804, 144
- Anderson, R. I., Mérand, A., Kervella, P., et al. 2016a, MNRAS, 455, 4231
- Anderson, R. I. 2016b, MNRAS, 463, 1707
- Anderson, R. I. 2014, A&A, 566, L10
- Anderson, R. I. 2019, A&A, 623, A146
- Ayres, T. 2011, ApJ, 738, 120
- Banyard, G., Sana, H., Mahy, L. et al. 2021, A&A, accepted
- Benedict, G. F., McArthur, B. E., Feast, M., et al. 2007, AJ, 133, 1810
- Berdnikov, L. N., Dambis, A. K., and Vozyakova, O. V. 2000, A&AS, 143, 211
- Berghoefer, T. W., Schmitt, J. H. M. M., Danner, R., and Cassinelli, J. P. 1997, A&A, 322, 167
- Bono, G., Marconi, M., Cassisi, S., et al. 2005, ApJ, 621,966
- Breuval, L 2021 PhD Thesis, Université Paris
- Chabrier, G. 2003, PASP, 115, 763
- Drilling, J. S. and Landolt, A. U. 2000 in Astrophysical Quantities, ed. A. N. Cox (New York: Springer), 381
- Engle, S. G., Guinan, E. F., Harper, G. M., et al. 2017, ApJ, 838, 67 (secret lives)
- Engle, S. G. 2015, PhD Thesis, James cook University
- Evans, N. R. 1992, ApJ, 384, 220
- Evans, N. R., Massa, D., and Proffitt, C. 2009, AJ, 137, 3700
- Evans, N. R., DeGoia-Eastwood, K., Gagné, M. et al. 2011, ApJS, 194, 13
- Evans, N. R., Bond, H. E., Schaefer, G. H., Mason, B. D., Karovska, M., and Tingle, E. 2013, AJ, 146, 93
- Evans, N. R., Berdnikov, L., Lauer, J. et al. 2015 AJ, 150, 13
- Evans, N. R., Pillitteri, I., Wolk, S., et al. 2016b, AJ, 151, 108
- Evans, N. R., Bond, H. E., Schaefer, G. H., et al. 2016a, AJ, 151, 129
- Evans, N. R. Karovska, M., Bond, H. E. et al. 2018, ApJ, 863, 187
- Evans, et al. 2020, AJ, 159, 121
- Evans, N. R., Guenther, H. M., Bond, H. E., et al. 2020a, ApJ, 905, 81

- Evans, N. R., Pillitteri, I., Kervella, P. et al. 2021, *AJ*, 162, 92
- Fernie, J. D., Evans, N. R., Beattie, B., and Seager, S. 1995, *IBVS*, 4148, 1
- Gallenne, A., M'erand, A., Kervella, P. et al. 2016, *MNRAS*, 461, 1451
- Gallenne, A., M'erand, A., Kervella, P. et al. 2021, *A&A*, 651, A113
- Gullikson, K., Kraus, A., and Dodson-Robinson, S. 2016, *AJ*, 152, 40
- Hocdé, V, et al. 2020a, *A&A*, 633, A47
- Hocdé, V, et al. 2020b, *A&A*, 641, A74
- Hocdé, V, et al. 2021, *A&A*, 651, A92
- Janson, M, Gratton, R. Roder, L. et al. 2022 arXiv:2112.04833
- Kervella, P., Arenou, F., and Thévenin, F. 2022, arXiv:2109.10902v2
- Kervella, P. Gallenne, A., Evans, N. R., et al 2019a, *A&A*, 623, A116
- Kervella, P., Gallenne, A., Evans, N. R. et al. 2019b, *A&A*, 623, A117
- Kobulnicky, H. A. and Fryer, C. L. 2007, *ApJ*, 670, 747
- Kouwenhoven, M. B. N., Brown, A. G. A., Portegies Zwart, S. F., and Kaper, L. 2007, *A&A*, 474, 77
- Merand, A. et al. 2006, *A&Ap*, 453, 155
- Meynet, G., Mermilliod, J.-C., and Maeder, A. 1993, *A&AS*, 98, 477
- Moe, M. and Di Stefano, R. 2017, *ApJS*, 230, 15
- Naze, Y., Broos, P., Oskinova, L. et al. 2011, *ApJS*, 215, 10
- Neilson, H. R., Engle, S. G., Guinan, E. F., Bisol, A. C., and Butterworth, N. 2016, *ApJ*, 824, 1
- Pillitteri, I., Evans, N. R., Wolk, S., and Syal, M. B. 2013 *AJ*, 145, 143 alp per
- Prebisch, T. and Feigelson, E. D. 2005, *ApJS*, 160, 390
- Randich, S., Schmitt, J. H. M. M., Prosser, C. F., and Stauffer, J. R. 1996, *A&A*, 305, 785
- Rizzuto, A. C., Ireland, M. J., Robertson, J. G., et al. 2013, *MNRAS*, 436, 1694
- Sana, H., de Mink, S. E., de Koter, A. et al. 2012, *Sci.*, 337, 444
- Seward, F. D. 2000, in *Astrophysical Quantities*, ed. A. N. Cox (New York: Springer), 381
- Stauffer, J. R., Barrado y Navascues, D. et al. 1999, *ApJ*, 527, 219
- Szabados, L. 1989, *Mitt. Sternwarte Ungar Akad Wissen.*, 94, 1
- Szabados, L. 1991, *Mitt. Sternwarte Ungar Akad Wissen.*, 96, 123
- Taylor, M. M., Albrow, M. D., Booth, A. J., and Cottrell, P. L. 1997, *MNras*, 292, 662
- Usenko, I. A., Kniazev, A. Yu., Berdnikov, L. N., Kravtsov, V. V., and Fokin, A. B. 2013, *AstL*, 39, 432
- Usenko, I. A., Kniazev, A. Yu., Berdnikov, L. N., Fokin, A. B. and Kravtsov, V. V. 2014, *AstL*, 40, 435
- Usenko, I. A., Kovtyukh, V. V., Miroshnichenko, A. S., and Danford, S. 2016, *OAP*, 29, 100